



Determination of the formation energy of edge, screw and twinning dislocations in fcc metals using the molecular dynamics

G.M. Poletaev ¹ ✉, R.Y. Rakitin ²

¹ Polzunov Altai State Technical University, Barnaul, Russia

² Altai State University, Barnaul, Russia

✉ gmpoletaev@mail.ru

Abstract. A method is proposed for determining the energy of moving edge, screw, and twinning dislocations in fcc metals using molecular dynamics, which consists in constructing and analyzing the graph of the time dependence of the potential energy of the calculation area of the crystal through which the dislocation passes. Nickel, copper, silver, and austenite are considered as examples of fcc metals. The initiation of the formation and movement of a dislocation was carried out by simulating a shear at a constant rate from the end of the computational cell. It was found that the shear rate above about 40 m/s affects the energy of dislocation: with increasing rate, the energy of the dislocation increases. According to the data obtained, the energy of an edge dislocation is approximately one and a half times higher than the energy of a screw dislocation. The energy of a twinning dislocation is much less than the energy of edge and screw dislocations. The moving twinning dislocation in the model was obtained as a result of the splitting of a screw dislocation on the twin into two partial dislocations that slide along the twin after splitting.

Keywords: molecular dynamics; metal; dislocation; dislocation energy; twinning dislocation

Citation: Poletaev GM, Rakitin RY. Determination of the formation energy of edge, screw and twinning dislocations in fcc metals using the molecular dynamics. *Materials Physics and Mechanics*. 2023;51(6): 84-91. DOI: 10.18149/MPM.5162023_8.

Introduction

The formation, motion, and interaction of dislocations with each other and with other defects are important questions, the search for answers to which is necessary for the development of theory of the mechanisms of plastic deformation of crystalline materials. The variety of crystalline systems, slip systems and types of dislocations, as well as options for the interaction of dislocations with other defects, gives rise to the complexity of this phenomenon.

Dislocations in metals are the subject of many works, including those performed using computer simulation [1–5]. In addition to complex issues of the interaction of dislocations with each other and with various defects, attention in modern works is also paid to relatively simple questions: for example, the dependence of the dislocation glide rate on temperature and strain rate [3,6]. As the strain rate increases, as is known, the dislocation velocity first increases and then reaches a certain limit, which, as a rule, is less than the speed of sound in a given material. Moreover, different authors give different values of this limit in relation to the speed of sound [3,6–8]. With increasing temperature, as noted by most researchers, the dislocation slip rate decreases [3,6,7].

Earlier in [9], using the method of molecular dynamics, the sliding of edge and screw dislocations in a fcc metal was studied using nickel and silver as an example, depending on the

temperature and shear rate, as well as the effect of impurity atoms of carbon, nitrogen, and oxygen on the sliding speed of dislocations.

This work is devoted to the determination of the energy of formation of edge, screw, and twinning dislocations in fcc metals (nickel, copper, silver, and austenite) using the molecular dynamics method.

Theoretically, the dislocation energy W per unit of its length l is determined by the formula [7,10]:

$$\frac{W}{l} = \frac{\mu b^2}{4\pi K} \ln \frac{R}{r_0}, \quad (1)$$

where μ is the shear modulus, b is the modulus of the Burgers vector, R is the radius of the computational area, and r_0 is the conditional radius. The parameter K depends on the type of dislocation: $K=1$ for a screw dislocation and $K=1-\nu$ for an edge one, where ν is Poisson's ratio.

The energy of a perfect edge dislocation is relatively high and can take values of 1–3 eV/Å for different metals [7,10,11]. Even in aluminum, with a relatively low binding energy of atoms, according to [11], the dislocation energy, depending on the orientation and the Burgers vector, can take values even up to several eV/Å.

Determination of the energy of edge and screw dislocations

To describe interatomic interactions in the metals under consideration, EAM potentials were used: Clery-Rosato [12] for modeling interactions in nickel, copper, and silver, and the Lau potential [13] for modeling interactions in γ -Fe. Both potentials have been repeatedly used in molecular dynamics models and have been successfully tested for a large number of structural, energy, and mechanical characteristics of the considered metals [12–16].

In fcc crystals, the $\{111\}\langle 110\rangle$ slip system is predominant [7, 8]. The Burgers vector of a complete dislocation is $1/2\langle 110\rangle$. A complete dislocation, as a rule, splits into two partial dislocations with Burgers vectors $1/6\langle 112\rangle$, between which a stacking fault is formed.

To simulate a moving dislocation, in this work, we created a computational cell containing about 30,000 atoms (Fig. 1) with axes oriented: X – $[\bar{1}10]$, Y – $[\bar{1}\bar{1}2]$, Z – $[111]$. The XY plane in this case corresponds to the dislocation glide plane (111). To initiate the movement of a dislocation, a shift was created from the end face of the computational cell [17,18]. Figure 1 shows the scheme for creating a moving perfect edge dislocation $\frac{1}{2}[\bar{1}01](111)$. The shaded regions from the left end moved as a whole along the directions shown in the figure: in the case of modeling an edge dislocation, the upper part of the end moved along the close-packed direction $[\bar{1}01]$, the lower part – along the opposite direction $[10\bar{1}]$. In the case of modeling a screw dislocation, the upper part was displaced along the $[\bar{1}10]$ direction (X axis), while the lower part was displaced along the $[1\bar{1}0]$ direction. Atoms inside the shaded region were displaced during computer simulation only along the indicated directions with a constant shear rate V_τ . The boundary conditions on this side were thus rigid. Along the X axis, along the dislocation core, the boundary conditions were set to be periodic, i.e. an infinite repetition of the structure of the computational cell along the X axis was simulated. For other boundaries, we used a special type of boundary conditions – conditionally rigid: all boundary atoms from above, below, and on the right had the ability to move only along the XY plane, movement along the Z axis was excluded. This was enough to keep, on the one hand, the given rectangular shape of the computational block and, on the other hand, the free exit of dislocations outside the computational cell.

The time integration step in the molecular dynamics method was 2 fs. The temperature in the model was set in terms of the initial velocities of the atoms according to the Maxwell distribution. A Nose-Hoover thermostat was used to keep the temperature constant during the simulation.

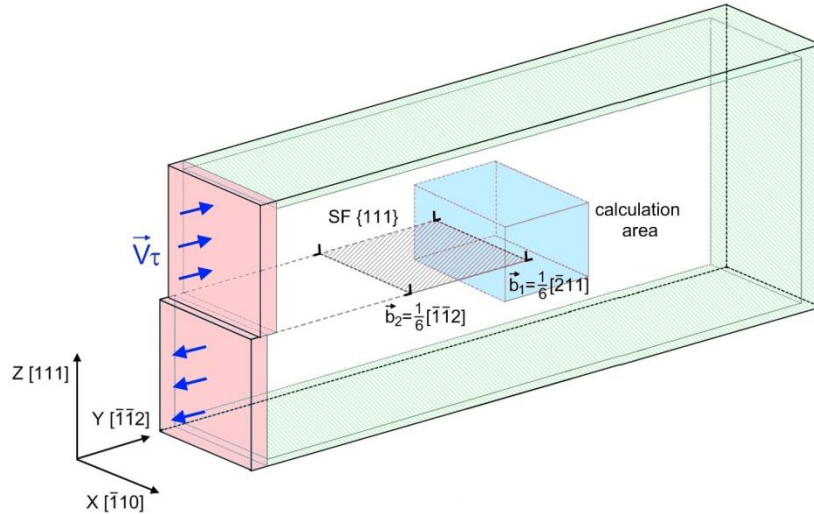


Fig. 1. To the description of the method for determining the energy of edge and screw dislocations

At some point in time, the shear in the left part of the computational cell provoked the appearance of a dislocation – edge or screw, depending on the shear direction. A dislocation appeared immediately in the form of a split into a pair of partial Shockley dislocations separated by a stacking fault in the (111) plane. For an edge dislocation, the splitting reaction had the form $\frac{1}{2} [\bar{1}01] \rightarrow \frac{1}{6} [\bar{2}11] + \frac{1}{6} [\bar{1}\bar{1}2]$, for screw dislocation – $\frac{1}{2} [\bar{1}10] \rightarrow \frac{1}{6} [\bar{1}2\bar{1}] + \frac{1}{6} [\bar{2}11]$. The distance between partial dislocations is known to be determined by the stacking fault energy [7,8]. In the present work, it was several nanometers (depending on the shear rate), which agrees with the results of modeling by other authors, for example [3–5].

During the movement of a dislocation through the calculation area (highlighted in color in the middle of the computational cell in Fig. 1), a graph of the change in the potential energy of the calculation area depending on time was plotted. The width of the calculation area was chosen such that, on the one hand, it was wider than the distance between partial dislocations (so that the entire complex of two partial dislocations could simultaneously fit in the calculation area) and, on the other hand, not so large that it could include part of the next dislocations. The temperature was set close to 0 K (more precisely, the starting temperature was 0 K, but in the process of creation and movement of the dislocation, the computational cell was heated to a low temperature of about 10 K).

First of all, in this work, we studied the effect on the obtained values of the energy of full dislocations (that is, the entire complex of two partial dislocations plus the stacking fault energy between them) of the width of the computational cell (the size along the X axis in Fig. 1) and the shear rate V_τ .

Figure 2 shows overlays of plots of changes in the specific energy of the calculation area ($\text{eV}/\text{\AA}$) during the passage of a full edge dislocation in pure FCC iron at different widths of the computational cell (Fig. 2(a)) and different shear rates (Fig. 2(b)).

As can be seen, starting from 8 interatomic distances (approximately 20 \AA), the width does not affect at all – the superimposed dependences repeat each other very well, the curves for different widths differ by no more than the value of ordinary fluctuations (it can be seen from the enlarged fragment in Fig. 2(a)). Up to 8 interatomic distances, as was shown in [16], the dislocation velocity can depend on the cell width.

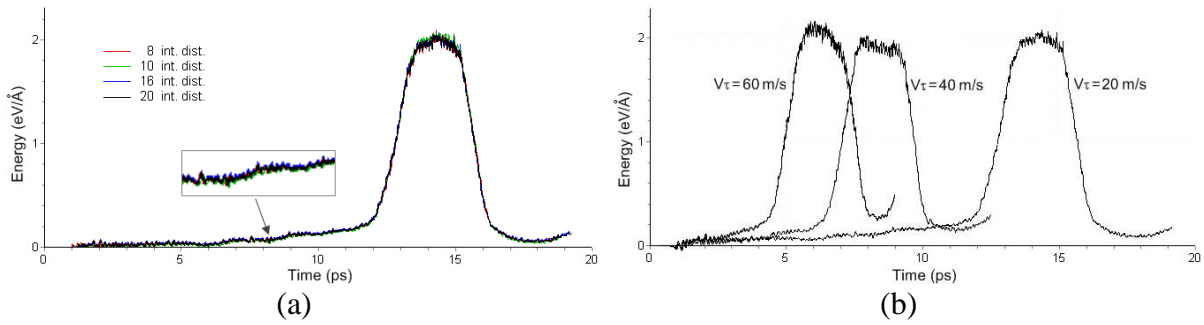


Fig. 2. Overlays of the change in the energy of the calculation area during the passage of an edge dislocation in γ -Fe: (a) at different widths of the computational cell (here, four graphs are superimposed at a width of 8, 10, 16, 20 interatomic distances); (b) at different shear rates (20, 40 and 60 m/s)

The shear rate V_τ , as it turned out, also has almost no effect on the height of the energy peak of the calculation area, but up to values of about 40–50 m/s. At a shear rate V_τ greater than 40–50 m/s, the energy slightly increases due to additional stresses and a smaller distance between neighboring dislocations. The velocity of the dislocations themselves also increases as they pass through the calculation area, which can be seen, for example, from the narrower peak for 60 m/s in Fig. 2(b). By the way, the dislocation velocity can also be determined from the width of this peak – this is another possible method for determining it. For the examples considered in the figure for austenite, its value was: 1500 m/s for a shear rate of 20 m/s, 1850 m/s for 40 m/s, and 2090 m/s for 60 m/s. In [19], we showed that with an increase in the shear rate, the dislocation slip velocity increases to a certain limit, which depends on the propagation velocity of the corresponding elastic waves: longitudinal in the case of an edge dislocation and transverse in the case of a screw one. For austenite, these are 5450 and 2865 m/s, respectively; for Ni, 5630 and 2960 m/s; for Cu, 4700 and 2260 m/s; for Ag, 3600 and 1590 m/s [8,10]. In further studies, the width of the computational cell was usually taken to be 10 or 12 interatomic distances.

Figure 3 shows a graph of the change in the energy of the calculation area for a screw dislocation in γ -Fe. It can be seen that the energy of a screw dislocation is noticeably lower than that of an edge one. The found energies of edge and screw dislocations in the metals under consideration are given below in the general table.

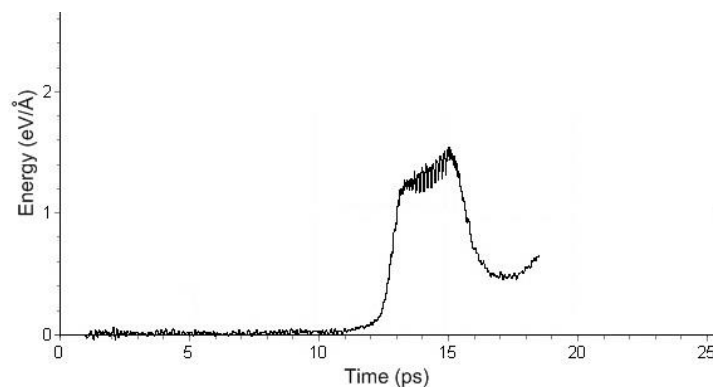


Fig. 3. Change in the energy of the calculation area during the passage of a screw dislocation in γ -Fe at a shear rate of 20 m/s

Determination of the energy of a twinning dislocation

Twinning dislocations are formed during the formation and migration of twins. As shown by molecular dynamics modeling in [16,20,21], when an edge dislocation overcomes a twin boundary and the slip plane changes, a twinning dislocation is formed at the boundary itself, which rapidly moves along the twin boundary, and if there is no obstacle to its movement, it "heals" the border [16]. The screw dislocation does not pass through the twin, but is absorbed by it, thus changing the glide plane [16,20,21]. This occurs at much lower stresses compared to edge dislocation. After changing the slip plane, both partial dislocations diverge in different directions along the twin boundary, "healing" the boundary, as in the case of the passage of an edge dislocation [16].

To calculate the energy of a twinning dislocation, it was assumed that the energy of twinning dislocations, which are formed during the passage of an edge dislocation and the splitting of a screw one, are the same. The method for determining the energy of a twinning dislocation resulting from the splitting of a screw dislocation at a twin boundary was as follows (Fig. 4). As in the case of an edge or screw dislocation, a similar graph was plotted for the change in the potential energy of the calculation area per unit of its width along the X axis in the process of splitting a screw dislocation on a twin. At the same time, to fix the moment of splitting of the screw dislocation on the twin, a graph of the displacement of the reference point located on the twin was displayed. The displacement of the reference point in this case was determined from the displacement relative to each other of two atoms located on opposite sides of the dislocation glide plane near the twin boundary. When splitting, which could be fixed by the peak of the displacement of the reference point, there was a slight decrease in the energy of the computational domain ΔE , caused by the disappearance of the stacking fault between partial dislocations. Partial dislocations changed the slip plane to the twin plane, which itself is, in fact, a stacking fault. The attraction between partial dislocations, which existed before the interaction with the twin and was due to the presence of a stacking fault, disappeared, which led to the repulsion of partial dislocations on the twin and their divergence in opposite directions (Fig. 4). The energy of a twinning dislocation was determined by the formula:

$$E_T = \frac{1}{2}(E_S - \Delta E), \quad (2)$$

where E_S is the energy of a perfect screw dislocation.

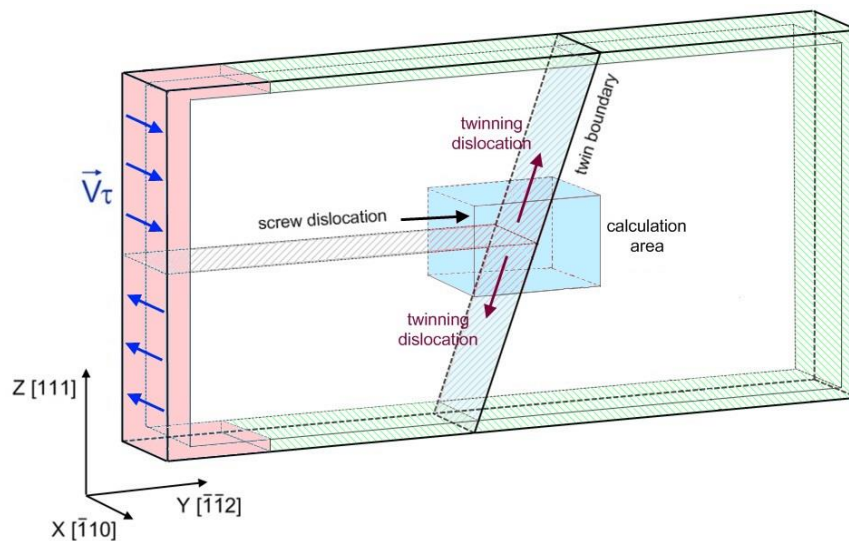


Fig. 4. To the description of the method for determining the energy of a twinning dislocation

Figure 5 shows an example of the change in the energy of the calculation area when a screw dislocation enters it and its subsequent splitting into two twinning dislocations. Comparing these graphs with the graphs of the passage of a screw dislocation through the calculation area in a pure crystal in Fig. 3, it should be noted that the width of the peaks is noticeably smaller, which means that the twinning dislocations leave the calculation area faster than the screw dislocation, i.e. they are more mobile, which was also noted in [16]. The Table 1 shows the obtained energies of edge, screw, and twinning dislocations.

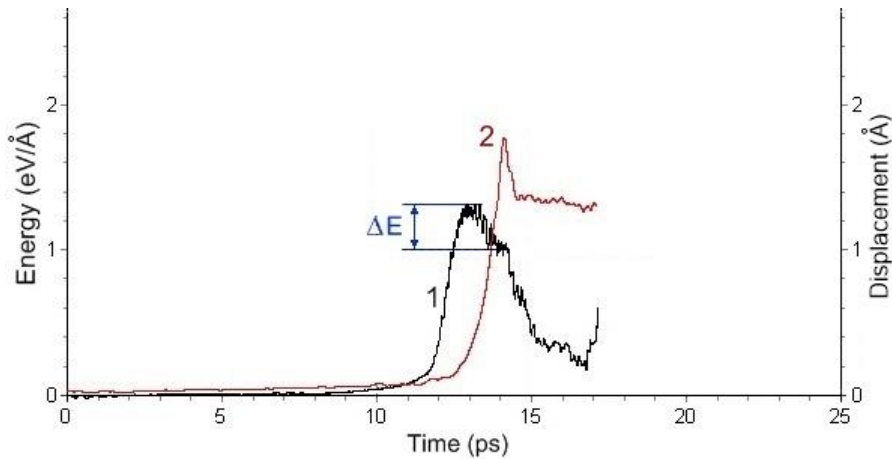


Fig. 5. Changes in the energy of the calculation area upon splitting of a screw dislocation into two twinning ones in γ -Fe at a shear rate of 20 m/s: 1 is the energy of the calculation area, 2 is the displacement of the reference atom on the twin boundary to determine the moment of splitting of the screw dislocation

Table 1. Edge, screw, and twinning dislocation energies in Ni, Cu, Ag, and γ -Fe (eV/Å)

	Edge	Screw	Twinning
Ni	1.7	1.1	0.4
Cu	1.0	0.6	0.2
Ag	0.7	0.5	0.2
γ -Fe	2.0	1.3	0.5

According to the data obtained, the energy of an edge dislocation is approximately one and a half times higher than the energy of a screw dislocation, which is consistent with theoretical formula (1). For the metals under consideration, the dislocation energies correlate with the elastic characteristics, which also agrees with formula (1). The energy of a twinning dislocation is substantially less than the energy of edge or screw dislocations. In fact, according to the method of obtaining it in the model, this is one of the partial dislocations that was formed during the splitting of a screw dislocation on a twin, so it should obviously be approximately two times lower than the energy of a full screw dislocation minus half the stacking fault energy between partial dislocations in the original screw dislocation.

Conclusion

A method is proposed for determining the energy of moving edge, screw, and twinning dislocations in fcc metals using molecular dynamics, which consists in constructing and analyzing the graph of the time dependence of the potential energy of the calculation area of the crystal through which the dislocation passes. Nickel, copper, silver, and austenite are considered as examples of fcc metals.

An edge or screw dislocation appeared in the simulation as a split into a pair of partial Shockley dislocations separated by a stacking fault. The distance between partial dislocations was several nanometers. At high shear rates, it decreased.

It was found that the shear rate affects the dislocation energy only up to values equal to approximately 40 m/s. At high velocities, the dislocation energy increases. In addition, it was found that, starting from 8 interatomic distances (approximately 20 Å), the width of the simulated computational cell with periodic conditions does not affect the obtained values of the dislocation energy.

According to the data obtained, the energy of an edge dislocation is approximately one and a half times higher than the energy of a screw dislocation. For the metals under consideration, the dislocation energies correlate with the elastic characteristics. The energy of a twinning dislocation is substantially less than the energy of edge or screw dislocations. The moving twinning dislocation in the model was obtained as a result of the splitting of a screw dislocation on the twin into two partial dislocations that slide along the twin after splitting.

References

1. Chen C, Meng F, Ou P, Lan G, Li B, Chen H, Qiu Q, Song J. Effect of indium doping on motions of $\langle a \rangle$ -prismatic edge dislocations in wurtzite gallium nitride. *Journal of Physics: Condensed Matter*. 2019;31(31): 315701.
2. Olmsted DL, Hector Jr LG, Curtin WA, Clifton RJ. Atomistic simulations of dislocation mobility in Al, Ni and Al/Mg alloys. *Modelling and Simulation in Materials Science and Engineering*. 2005;13(3): 371–388.
3. Zhao Sh, Osetsky YuN, Zhang Y. Atomic-scale dynamics of edge dislocations in Ni and concentrated solid solution NiFe alloys. *Journal of Alloys and Compounds*. 2017;701: 1003–1008.
4. Rodney D, Ventelon L, Clouet E, Pizzagalli L, Willaime F. Ab initio modeling of dislocation core properties in metals and semiconductors. *Acta Materialia*. 2017;124: 633–659.
5. Hunter A, Beyerlein IJ, Germann TC, Koslowski M. Influence of the stacking fault energy surface on partial dislocations in fcc metals with a three-dimensional phase field dislocations dynamics model. *Physical Review B*. 2011;84(14): 144108.
6. Po G, Cui Y, Rivera D, Cereceda D, Swinburne TD, Marian J, Ghoniem N. A phenomenological dislocation mobility law for bcc metals. *Acta Materialia*. 2016;119: 123–135.
7. Friedel J. *Dislocations*. Oxford: Pergamon press; 1964.
8. Hirth JP, Lothe J. *Theory of Dislocations*. 2nd ed. NY: Wiley; 1982.
9. Poletaev GM, Zorya IV. Effect of light element impurities on the edge dislocation glide in nickel and silver: molecular dynamics simulation. *Journal of Experimental and Theoretical Physics*. 2020;131(3): 432–436.
10. Cahn RW, Haasen P. *Physical Metallurgy*. 3th ed. Amsterdam: North-Holland Physics Publishing; 1983.
11. Zhou XW, Sills RB, Ward DK, Karnesky RA. Atomistic calculations of dislocation core energy in aluminium. *Physical Review B*. 2017;95(5): 054112.
12. Cleri F, Rosato V. Tight-binding potentials for transition metals and alloys. *Physical Review B*. 1993;48(1): 22–33.
13. Lau TT, Forst CJ, Lin X, Gale JD, Yip S, Van Vliet KJ. Many-body potential for point defect clusters in Fe-C alloys. *Physical Review Letters*. 2007;98(21): 215501.
14. Lv B, Chen C, Zhang F, Poletaev GM, Rakitin RY. Potentials for describing interatomic interactions in γ Fe-Mn-C-N system. *Metals*. 2022;12(6): 982.
15. Poletaev GM. Self-diffusion in liquid and solid alloys of the Ti–Al system: molecular-dynamics simulation. *Journal of Experimental and Theoretical Physics*. 2021;133(4): 455–460.

16. Chen C, Zhang F, Xu H, Yang Z, Poletaev GM. Molecular dynamics simulations of dislocation–coherent twin boundary interaction in face-centered cubic metals. *Journal of Materials Science*. 2022;57: 1833–1849.
17. Poletaev GM, Rakitin RY. Molecular dynamics study of stress-strain curves for γ -Fe and Hadfield steel ideal crystals at shear along the $\langle 111 \rangle$ direction. *Materials Physics and Mechanics*. 2021;47(2): 237–244.
18. Poletaev GM, Rakitin RY. Molecular dynamics simulation of severe plastic deformation of nanotwinned Hadfield steel. *Materials Physics and Mechanics*. 2022;50(1): 118–125.
19. Zorya IV, Poletaev GM, Rakitin RY. Energy and velocity of sliding of edge and screw dislocations in austenite and Hadfield steel: molecular dynamics simulation. *Steel in Translation*. 2022;52(12): 1121–1126.
20. Jin Z-H, Gumbsch P, Ma E, Albe K, Lu K, Hahn H, Gleiter H. The interaction mechanism of screw dislocations with coherent twin boundaries in different face-centred cubic metals. *Scripta Materialia*. 2006;54(6): 1163–1168.
21. Chassagne M, Legros M, Rodney D. Atomic-scale simulation of screw dislocation/coherent twin boundary interaction in Al, Au, Cu and Ni. *Acta Materialia*. 2011;59(4): 1456–1463.

THE AUTHORS

Poletaev G.M. 

e-mail: gmpoletaev@mail.ru

Rakitin R.Y. 

e-mail: movehell@gmail.com